PERGAMON

Chemical Engineering Science 55 (2000) 3885–3897

Chemical Engineering Science

Start-up and wrong-way behavior in a tubular reactor: dilution effect of the catalytic bed

Margarida M. J. Quina, Rosa M. Quinta Ferreira*

Department of Chemical Engineering, University of Coimbra, 3000 Coimbra, Portugal

Abstract

The start-up and the wrong-way behavior of a fixed-bed reactor were analyzed through one-dimensional heterogeneous and pseudo-homogeneous models. The simulation work was based on the methanol oxidation to formaldehyde, which takes place in a fixed-bed reactor with two distinct zones. In the first part of the reactor, the catalyst was diluted with inert, and in the second zone the catalyst is pure. This activity profile leads to new features on the start-up and wrong-way behavior of the system when compared with a uniform catalytic bed. For a partially diluted bed, when the inlet temperature is increased (decreased), the final steady state can show a hot spot lower (higher) than the initial one. This behavior is not observed in a one-zone bed, where the final steady-state maximum temperature is always higher (lower) than the initial one if the inlet temperature is submitted to a positive (negative) change. During the dynamic period, the transient profiles are closer to the initial steady states in the case of the two-zone bed, pointing out that the catalyst dilution in the upstream section of the reactor can decrease the system sensitivity in both steady state and dynamic period. The differences between the predictions obtained through the pseudo-homogeneous and the heterogeneous models can be more significant on the transient responses than on the steady state situations and the wall temperature is the most important parameter on the reactor dynamic response. Moreover, significant wrong-way behavior can occur for step changes and ramp variations in feed and wall temperatures.

Keywords: Packed bed; Catalyst dilution; Mathematical modeling; Dynamic simulation; Transient response; Wrong-way behavior

1. Introduction

There are some features associated with the behavior of fixed-bed reactors that can only be revealed through transient analysis. In fact, the dynamic response of the reactor may have surprising characteristics which can lead to control failures, deactivation of the catalyst, problems during the start-up and shut-down, etc. Therefore, the design of the control systems and the start-up and shut-down procedures should be preceded by an analysis of the transient behavior.

The start-up of the system is dominated by the competition between two physical phenomena: the propagation of the mass wave, which is very fast, and the velocity of the thermal wave, which is very slow. Therefore, after a time equal to the space time for the fluid, L/u_i, a pseudo-steady state is reached, which is similar to an isothermal operation. Afterwards, a long period is needed to obtain the final steady state. Quinta Ferreira, Costa and Rodrigues (1992, 1996) dedicated particular attention to the start-up of fixed-bed reactors, and have studied different mathematical strategies for solving several types of dynamic models. The intraparticle convection effects have also been emphasized. Zheng and Gu (1996) obtained an analytical solution for the start-up period through the Laplace transform, using a one-dimensional model including terms of axial dispersion and assuming an isothermal process. The predictions obtained fitted quite well with the experimental results. Verwijs, van den Berg and Westerterp (1992, 1994) Verwijs, Koster van der Berg and Westerterp (1995) have also shown experimental results of the start-up reactor and simulated failures and demonstrated that the start-up period determines the future steady-state operation of the reactor. Lopéz-Isunza (1983) has observed that for the partial oxidation of the *o*-xylene to phthalic anhydride, a heterogeneous model fitted well with the steady-state experimental results but not the transient behavior. He concluded that for the transient case it was important to take into

* Corresponding author. Tel.: +351-239798700; fax: +351-239798703.

E-mail address: eq1rqf@eq.uc.pt (R. M. Quinta Ferreira)

0009-2509/00/$ - see front matter
PII: S0009-2509(00)00029-4

account the deactivation of the catalyst. Windes, Schwedock and Ray (1989) have stressed that the steady-state models are usually used for design purposes, kinetic studies and parameters estimation, and the dynamic models are important to design control devices. Their study was also based on the partial oxidation of methanol to formaldehyde, and the predictions of different types of mathematical models have shown that even when the steady-state results are in good qualitative agreement, the transient results obtained with pseudo-homogeneous and heterogeneous models can be substantially different in some cases.

The wrong-way behavior can occur when a sudden change (increase or decrease) in an inlet variable leads initially to an unexpected variation on the hot spot temperature of the system. This behavior is due to the high velocity of the mass wave in respect to the velocity of propagation of the thermal wave through the fixed-bed reactor, which is related to the higher thermal capacity of the solid phase when compared with the thermal capacity of the gas phase. Sinai and Foss (1970), among others, have demonstrated that the thermal wave controls all the dynamic responses of the fixed-bed reactors. Kulkarni and Dudukovic (1996, 1998) give a more complete explanation of the wrong-way behavior of a fixed-bed reactor based on the magnitude of the heat transfer time scale, τ_{hf}, and the reaction time scale, τ_r. According to those authors, a low τ_{hf} relative to τ_r indicates a considerable increase of the temperature of the reactants before appreciable reaction takes place, leading to wrong-way behavior of the fixed-bed reactor.

The wrong-way behavior was first predicted by Crider and Foss (1966), and since then several studies have been published. McGreavy and Naim (1977) and Windes et al. (1989) studied this subject through one and two-dimensional mathematical models. Metha, Sams and Luss (1981) found analytical criteria to predict that behavior, for zero-order reactions. Pinjala, Chen and Luss (1988) analyzed the importance of the thermal dispersion on the transient response, and concluded that the ignition of the reactor during the transient period is possible to occur. They suggested that axial dispersion terms should be included in the mathematical models, when the transient response of the system is studied. Chen and Luss (1989) investigated the influence of the intraparticle resistances on the wrong-way behavior. Il'in and Luss (1992) have shown how the reactant adsorption on the inert catalyst support may affect that behavior, and later on the same authors (Il'in & Luss, 1993) showed the impact on wrong-way behavior of an undesired consecutive reaction. They concluded that in this case, due to the temperature rise, a loss of yield of the desired product can be observed. Almeida-Costa, Quinta Ferreira and Rodrigues (1994) investigated the impact of the intraparticle convection on wrong-way behavior. Kulkarni and Dudukovic (1996) studied the dynamics of a fixed-bed reactor where reaction takes place in both gas and solid phases.

Experimentally, the wrong-way behavior was observed by Hoiberg, Lyche and Foss (1971), Van Doesburg and De Jong (1976) Sharma and Hughes (1979a, b) and Lopéz-Isunza (1983), among others. Under some circumstances this behavior can lead to undesired results, such as promotion of side reactions, catalyst deactivation and thermal runaway. Moreover, if the system operates in a multiplicity zone, the increase of the temperature during the transient period can lead to a jump from a lower-temperature steady-state to a higher-temperature steady-state (Sharma & Hughes, 1979b; Pinjala, Chen & Luss, 1988), which is known as the ignition of the reactor.

The main objective of this work is to study the effect of two zones with different catalytic activities on the transient behavior of a fixed-bed reactor in two different situations: start-up period and dynamic behavior to step and ramp changes in some inlet variables (feed temperature, feed concentration, wall temperature, feed and wall temperatures simultaneously). The industrial system of partial oxidation of methanol to formaldehyde over iron/molybdenum oxides catalysts has been selected as a case study. The process takes place at atmospheric pressure and the feed temperature is 530 K.

The modeling process considers a single-tube reactor, which is divided in to two zones: a less active bed at the inlet (with a length of 0.2 m) where the catalyst is diluted with 50% inert, followed by a second zone with pure catalyst (0.55 m). This leads to a moderate heat production and consequently a smoother transient behavior when compared to uniform-activity reactors.

According to Bucalá, Borio, Romagnoli and Porras (1992), Harris, Mac Gregor and Wright (1980) and Alvarez, Romagnoli and Stephanopoulos (1981), in a fixed-bed reactor, the temperature sensor should be located before the hot spot region. Therefore, also in this study we have considered the zone of the hot spot as the reference one. As it will be shown in the next sections, the presence of two distinct catalytic zones can lead to surprising situations, such as the decrease of the final hot-spot temperature after a positive change in the inlet temperature.

2. Mathematical models

In our system, the main reaction is the partial oxidation of methanol to formaldehyde ($CH_3OH + \frac{1}{2}O_2 \rightarrow CH_2O + H_2O$), and through an undesirable consecutive reaction the carbon monoxide is also produced by the partial oxidation of the formaldehyde ($CH_2O + \frac{1}{2}O_2 \rightarrow CO + H_2O$). The kinetic model chosen to describe the first reaction, R_1, was proposed by Dente, Collina and Pasquon (1966):

$$R_1 = k_1(T)P^{0.75}Y_M^{0.75}/(1 + Y_M^{0.75})^{0.5},$$

where $k_1(T) = k_{o,1}e^{-E_{a,1}/RT}$, with $k_{o,1} = 2.29 \times 10^2$ mol/kg_{cat} s $atm^{0.75}$ and $E_{a,1} = 36786$ J/mol.

For the second reaction the kinetic model was proposed by Dente and Collina (1965):

$$R_2 = k_2(T)P_{CH_2O},$$

where $k_2(T) = k_{o,2}e^{-E_{a,2}/RT}$, with $k_{o,2} = 3.0 \times 10^3$mol/$kg_{cat}$ .s. atm and $E_{a,2} = 66413$ J/mol.

In this work, the dynamic behavior of the reactor was studied through a one-dimensional pseudo-homogeneous model, PH1DT, and a one-dimensional heterogeneous model (HT1DT), both including axial mass and heat dispersion. In both cases, we have assumed constant wall temperature, constant physical properties and no radial profiles. According to Pinjala et al. (1988) and Chen and Luss (1989), when the inlet variables are changed, if axial dispersion is not taken into account, discontinuities in state variables will be observed, which do not correspond to the physical reality. On the other hand, the terms of axial dispersion allow the transformation of hyperbolic partial differential equations into parabolic partial differential equations, which are much easier to solve.

2.1. One-dimensional transient pseudo-homogeneous model, PH1DT

The dimensionless equations for the dynamic pseudo-homogeneous model are shown in Table 1. The dimensionless model parameters were calculated at the reference conditions ($T_o = 530$ K, $P_o = 1$ atm, $C_{M,o} = 2.4$ mol/m^3): $Pe_{ma} = 644$; $Pe_{ha} = 145$; $\tau/\tau_{hl} = 6.730 \times 10^{-4}$; $N_w = 11.49$; $Da = 1.04\ (2.08)$; $B_1 = 0.729$; $B_2 = 1.071$; $\theta_w = 1.0$. The Peclet numbers based on the catalyst diameter are $Pe_{ma}(d_{pe}) = 2$ and $Pe_{ha}(d_{pe}) = 0.45$, and the space times for the fluid and thermal wave are $\tau = L/u_i = 0.203$ s; $\tau_{hl} = \tau[(1-\varepsilon_b)\rho_s Cp_s + \varepsilon_b \rho_f Cp_f]/\varepsilon_b \rho_f Cp_f = 302$ s. The Damköhler number is 1.04 on the first zone where the catalyst is diluted with 50% of inert particles ($\rho_b = 550$ kg/m^3 for $0 \leqslant z \leqslant 0.2$ m) and 2.08 on the second zone with pure catalyst ($\rho_b = 1100$ kg/m^3 for $0.2 \leqslant z \leqslant 0.75$ m).

2.2. One-dimensional transient heterogeneous model, HT1DT

The transient heterogeneous models are based on some common assumptions: the catalyst particle was considered isothermal (Hansen, 1971, 1973), and the concentration profiles inside the catalyst were assumed to be in pseudo-steady-state (Ferguson & Finlayson, 1974; Quinta Ferreira et al., 1992, 1996). The catalyst particle was assumed to have slab geometry, where in addition to the intraparticle diffusion, the mass transport by convection could also be accounted for. The dimensionless transient equations are shown in Table 2, and the parameters were calculated using the previous reference conditions: $Pe_{ma} = 644$; $Pe_{ha} = 145$; $\tau/\tau_h = 6.734 \times 10^{-4}$; $N_w = 11.49$; $Nf_M = 95.5$; $Nf_F = 100.4$; $Nf_h = 118.7$; $Da = 1.04\ (2.08)$; $B_1 = 0.729$; $B_2 = 1.071$; $\theta_w = 1.0$; $\phi_{M,o} = 0.57$; $\phi_{F,o} = 0.55$; $\lambda_{m,i} = 0$ (if only intraparticle diffusion is considered — $HT1DT_d$ model) and $\lambda_{m,i} = 10$ (when intraparticle diffusion and convection are taken into account — $HT1DT_{dc}$ model). Once again the Damköhler number is 1.04 on the first zone and 2.08 on the second zone.

τ being the space time for the fluid and τ_h the space time for the thermal wave, τ_h/τ represents the ratio between the velocity of propagation of the mass wave and that of the thermal wave, when there is no reaction. For our system, $\tau = L/u_i = 0.203$ s; $\tau_h = \tau\ [(1-\varepsilon_b)\rho_s Cp_s]/\varepsilon_b \rho_f Cp_f = 301$ s, and therefore $\tau_h/\tau \cong 1500$. This indicates that the high thermal inertia of the solid packing will retard the temperature front along the bed in respect to the mass front. As a consequence, higher (or lower) maximum transient temperatures will develop for lower (or higher) feed temperatures revealing a wrong-way behavior of the system. A more complete explanation of the

Table 1
Dimensionless equations for the dynamic pseudo-homogeneous model, PH1DT[a]

Mass balance: $$\frac{\partial f_i}{\partial t^*} = -\frac{\partial f_i}{\partial z^*} + \frac{1}{Pe_{ma}}\frac{\partial^2 f_i}{\partial z^{*2}} + Da\sum_{j=1}^{2}\alpha_{i,j}\Re_j \quad (1)$$

Energy balance: $$\frac{\partial \theta}{\partial t^*} = \frac{\tau}{\tau_{hl}}\left\{-\frac{\partial \theta}{\partial z^*} + \frac{1}{Pe_{ha}}\frac{\partial^2 \theta}{\partial z^{*2}} + Da\sum_{j=1}^{2}B_j\Re_j + N_w(\theta_w - \theta)\right\} \quad (2)$$

$$i = CH_3OH,\ CH_2O$$

Initial conditions: $t^* = 0; f_i(z^*,0) = f_{i,o}(z^*); \theta(z^*,0) = \theta_o(z^*)$ (3a)

Boundary conditions: $z^* = 0; f_i(0,t^*) = C_{i,o}(t^*)/C_{M,o}(t^*); \theta(0,t^*) = 1$ (3b)

$$z^* = 1; \frac{\partial f_i(1,t^*)}{\partial z^*} = 0; \quad \frac{\partial \theta(1,t^*)}{\partial z^*} = 0 \quad (3c)$$

[a]Model parameters: $B_j = (-\Delta H)_j C_{M,o}/\rho_f Cp_f T_o$; $Da = L\rho_b R_{1,o}/u_o C_{M,o}$; $N_w = 4UL/d_t \rho_f Cp_f u_o$; $Pe_{ha} = Lu_o \rho_f Cp_f/\lambda_{ea}$; $Pe_{ma} = Lu_o/D_{ea}$; $\theta_w = T_w/T_o$; $\tau = L/u_i$; $\tau_{hl} = \tau[(1-\varepsilon_b)\rho_s Cp_s + \varepsilon_b \rho_f Cp_f]/\varepsilon_b \rho_f Cp_f$.

Table 2
Dimensionless equations for the dynamic heterogeneous model, HT1DT[a]

Fluid phase

Mass balance: $$\frac{\partial f_{i,b}}{\partial t^*} = -\frac{\partial f_{i,b}}{\partial z^*} + \frac{1}{Pe_{ma}}\frac{\partial^2 f_{i,b}}{\partial z^{*2}} - Nf_i(f_{i,b} - f_{i,s}) \quad (4)$$

Energy balance: $$\frac{\partial \theta_b}{\partial t^*} = -\frac{\partial \theta_b}{\partial z^*} + \frac{1}{Pe_{ha}}\frac{\partial^2 \theta_b}{\partial z^{*2}} + Nf_h(\theta_s - \theta_b) + N_w(\theta_w - \theta_b)i = \mathrm{CH_3OH,CH_2O} \quad (5)$$

Initial conditions: $t^* = 0; f_{i,b}(z^*,0) = f_{i,bo}(z^*); \theta_b(z^*,0) = \theta_{bo}(z^*)$ (6a)

Boundary conditions: $z^* = 0; f_{i,b}(0,t^*) = C_{i,bo}(t^*)/C_{M,o}\,(t^*); \theta_b(0,t^*) = 1$ (6b)

$$z^* = 1; \frac{\partial f_{i,b}(1,t^*)}{\partial z^*} = 0; \frac{\partial \theta_b(1,t^*)}{\partial z^*} = 0 \quad (6c)$$

Interface fluid/particle

Mass balances: $$-Nf_i(f_{i,b} - f_{i,s}) = Da\sum_{j=1}^{2}\alpha_{i,j}\Re_j^s\eta_j \quad (7)$$

Energy balance: $$\frac{\mathrm{d}\theta_s}{\mathrm{d}t^*} = \frac{\tau}{\tau_h}\left\{Da\sum_{j=1}^{2}B_j\Re_j^s\eta_j - Nf_h(\theta_s - \theta_b)\right\} \quad (8)$$

Initial condition: $t^* = 0;\ \theta_s(z^*,0) = \theta_{so}(z^*)$ (8a)

Catalyst particle

Mass balance: $$\frac{\mathrm{d}^2 f_{i,p}}{\mathrm{d}r_p^{*2}} - 2\lambda_{m,i}\frac{\mathrm{d}f_{i,p}}{\mathrm{d}r_p^*} + 4\phi_{i,o}^2\sum_{j=1}^{2}\alpha_{i,j}\Re_j^p = 0 \quad (9)$$

Boundary conditions: $r_p^* = 0; f_{i,p} = f_{i,s};\quad r_p^* = 1; f_{i,p} = f_{i,s}$ (10)

Effectiveness factors: $$\eta_j = \frac{\int_0^1 R_j^p(f_{i,p})\,\mathrm{d}r_p^*}{R_j^s(f_{i,s})} \quad \text{with } j = 1, 2 \quad (11)$$

[a]Model parameters: $B_j = (-\Delta H)_j C_{M,o}/\rho_f Cp_f T_o$: $Da = L\rho_b R_{l,o}/u_o C_{M,o}$; $Nf_h = h_f a_v L/u_o\rho_f Cp_f$; $Nf_i = k_{f,i}a_v L/u_o$; $N_w = 4UL/d_t\rho_f Cp_f u_o$; $Pe_{ha} = Lu_o\rho_f Cp_f/\lambda_{ea}$; $Pe_{ma} = Lu_o/D_{ea}$; $\theta_w = T_w/T_o$; $\phi_{i,o} = R_p\sqrt{\rho_p R_{1,o}/D_{e,i}C_{M,o}}$; $\lambda_{m,i} = v_o R_p/D_{e,i}$ $\tau = L/u_i$; $\tau_h = \tau(1-\varepsilon_b)\rho_s Cp_s/\varepsilon_b\rho_f Cp_f$.

wrong-way behavior of the fixed-bed reactor is given by the magnitude of the heat transfer time scale and the reaction time scale, as referred by Dudukovic and co-workers (Kulkarni & Dudukovic, 1996, 1998). In our dimensionless model equations, the heat transfer between the gas and solid is represented by the Number of film heat transfer units, N_{fh}, which can be considered as the ratio between the space time, τ, and the film heat transfer time scale, τ_{hf}: $N_{fh} = h_f a_v L/u_o\rho_f Cp_f = \tau/\tau_{hf}$, where $\tau_{hf} = \rho_f Cp_f\varepsilon_b/h_f a_v$. The Damköhler number, Da, represents the ratio between the space time, τ, and the reaction time scale, τ_r: $Da = L\rho_b R_{1,o}/u_o C_{M,o} = \tau/\tau_r$, where $\tau_r = \varepsilon_b C_{M,o}/\rho_b R_{1,o}$. At standard inlet conditions ($T_o = 530$ K; $C_{M,o} = 2.414$ mol/m^3) $\tau_{hf} = 0.0017$ s, $\tau_r = 0.194$ s (for the diluted section) and $\tau_r = 0.097$ s (for the non-diluted section), being then the heat transfer time scale much lower than the reaction time. As stated by Kulkarni & Dudukovic (1996; 1998) a low τ_{hf} in relation to τ_r will lead to the wrong-way behavior of the fixed-bed reactor.

In some simulations, the convective flow within the pellet was also taken into account and was compared to the case where internal diffusion is the only transport mechanism. The competition between these two mechanisms of transport is represented by the intraparticle mass Peclet number, $\lambda_{m,i} = v_o R_p/D_{e,i}$, which is defined as the ratio of the intraparticle convection to the intraparticle diffusion. In terms of time scale, a time constant can also be defined for pore diffusion, $\tau_{d,i} = \varepsilon_p R_p^2/D_{e,i}$ as well as for intraparticle convection, $\tau_c = \varepsilon_p R_p/v_o$, being then the intraparticle Peclet number defined as the ratio between the diffusive and convective times, $\lambda_{m,i} = \tau_{d,i}/\tau_c$.

The effectiveness factors for each reaction j ($j = 1, 2$) at each axial position, z^* and time, t^*, are given by (11), where the intraparticle concentration profiles are obtained by solving (9) and (10).

2.3. Numerical methods

As referred before, the inclusion of axial dispersion terms on the transient equations renders the models more realistic and the hyperbolic equations are transformed into parabolic equations, which are easier to solve. In this case, the pseudo-homogeneous and the heterogeneous models were solved by using the PDECOL package (Madsen & Sincovec, 1975), which allows the solution of PDEs (partial differential equations), by discretizing the axial coordinate through the

method of orthogonal collocation on finite elements. In this work, finite elements with different lengths were used along the reactor, in order to concentrate a higher number of collocation points in the zones where the variables had stronger variations, namely in the transition zone of the catalytic bed. This procedure allows the reduction or even the elimination of numerical oscillations. For the heterogeneous model, the algebraic equations (Eq. (7), Table 2) were solved through an iterative procedure.

The state variables related with the particle surface conditions have a discontinuity (T_s, $C_{M,s}$ and $C_{F,s}$), due to an increase of the bulk density, ρ_b, on the transition of the first zone to the second one, and it was then necessary to have some precautions on the discretization process of the axial coordinate. Since the orthogonal collocation method involves a continuity criterion, we have forced that one boundary of a finite element was coincident with the transition axial coordinate $z = 0.2$ m, and then all the dependent parameters are continuous across the discontinuous boundary.

For the pseudo-homogeneous model, the number of finite elements used to discretize the axial coordinate of the reactor was not a critical parameter, since the solution of the problem was very fast (using 34 finite elements, the CPU time in a SUN SPARC 10/52 computer was 3 s). However, for the heterogeneous model the CPU time is strongly dependent on the number of discretization points, since Eq. (9) has to be solved for each axial position and time. One could conclude that 14 finite elements for Eqs. (4), (5), (6a), (7) and (8) and 4 finite elements for Eq. (9) were a good compromise between the quality of the solution and the CPU time (Quina & Quinta Ferreira, 1998). Our results showed that the relation between the CPU time and the number of finite elements is not linear. In fact, in some cases a lower number of finite elements can require a higher computation time due to the difficulty for representing the sharp concentration fronts. Therefore, the number of finite elements to be used in the discretization process must be optimized.

3. Computer results

The dynamic behavior of the reactor will be analyzed through start-up and transient responses to step and ramp changes in some inlet variables.

3.1. Start-up period

The start-up process was simulated by changing the feed concentration from 0 to 2.4 mol/m^3, assuming the reactor to be initially heated at the cooling fluid temperature, T_w. Fig. 1(a) and (b) show the temperature and methanol concentration profiles predicted by the

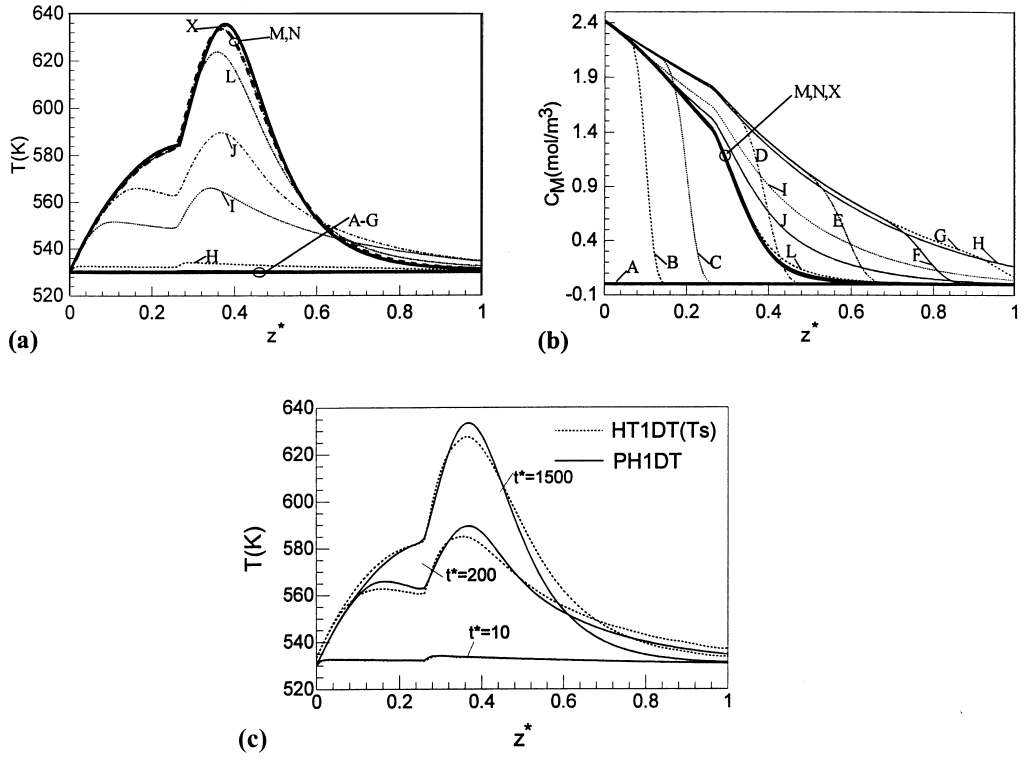

Fig. 1. Start-up of the reactor predicted with PH1DT model, by changing the inlet concentration from 0 to 2.4 mol/m^3. (a) Axial temperature profiles; (b) axial profiles of the methanol concentration for different dimensionless times $t^*(=t/\tau)$: A-0.; B-0.1; C-0.2; D-0.4; E-0.6; F-0.8; G-1.0; H-10.0; I-100.; J-200.; L-500.; M-1000.; N-1500.; X-steady state obtained with a model without axial dispersion; (c) comparison between PH1DT and HT1DT$_d$ models for $t^* = 10$; 200 and 1500.

pseudo-homogeneous model, for different dimensionless times. The propagation velocity of the concentration wave is higher than the one of the temperature wave; therefore, during the transient period two distinct situations occur. Due to the high heat capacity of the catalyst, the heat released by reaction is firstly absorbed by the solid and the temperature remains quite constant. The reactor exhibits then a pseudo-isothermal behavior with sharp mass fronts along the bed. After a dimensionless time $t^* = 10$, a hot spot begins to develop in each zone, due to the heat released by reaction (Fig. 1(a)), and the methanol concentration decreases, Fig. 1(b). After a dimensionless time of 1500, the system reaches a new steady-state (all the axial profiles are coincident). One can observe that the steady-state obtained by using a model with axial dispersion terms (curves M and N) is nearly coincident with that obtained when this phenomenon is neglected (curves X). Curves N were then considered as the initial steady-state of the transient responses of the system to several changes in inlet variables in the following analysis.

In Fig. 1(c), some transient temperature profiles predicted by the two models, PH1DT and $HT1DT_d$ can be compared and it can be seen that during the transient period, the hot spots for the heterogeneous model are also lower than the ones obtained with the pseudo-homogeneous model.

3.2. Transient response to step and ramp changes in inlet variables — wrong-way behavior

The reactor dynamic behavior was predicted by simulating step changes in some operating variables, such as feed temperature, feed concentration, wall temperature and feed and wall temperatures simultaneously.

For comparison purposes, Fig. 2 show the dynamic responses to a step change in the feed temperature for a reactor packed only with pure catalyst. A step up in feed temperature (from 530 to 557 K), represented in Fig. 2(a), results initially in a decrease on the hot spot (curves B–E) and later in an increase (curves F–I). Curves A and I correspond to the initial and final steady states, respectively. For a step down in T_o, Fig. 2(b) shows that the hot-spot temperature rises initially (curves B–E), decreasing afterwards (curves F–I) until the final steady state. This is the well known "wrong-way behavior": in the first times of the transient responses, the hot spot temperature decreases after a positive step, and increases after a negative step.

Imposing the same disturbance in a reactor with two different catalytic zones (a first zone with catalyst diluted with 50% inert packing and a second zone with pure catalyst) a wrong-way behavior was also detected, showing some new features. A step up in feed temperature, depicted in Fig. 3(a), leads to an initial reduction of the hot spot in an inner zone of the reactor (curves C–F), when compared with the initial steady-state profile (curve A), followed afterwards by a temperature rise (curves G–I). However, these hot spots stay lower than the initial value. This is not the case when the system is packed only with pure catalyst, where an increase of the feed temperature will also increase the final steady-state maximum temperature, which is located closer to the entrance of the reactor (Fig. 2(a), curve I). In such case, a higher reaction rate will lead to a faster reactant consumption in the inlet region of the reactor and the lower quantity of reactant further in the bed will then decrease the reaction rate and the system temperature.

For partially diluted beds, when the reaccional mixture enters the system at a higher temperature, a global temperature increase inside the reactor will also occur, involving a higher consumption of the reactants in the first zone. However, the lower amount of reactant on the second zone can lead to a decrease of the final steady-state temperature (curve I) below the previous maximum value (curve A), as observed in Fig. 3(a). So, when the catalytic bed has different activities along the reactor, one cannot foresee an increase of the hot-spot temperature

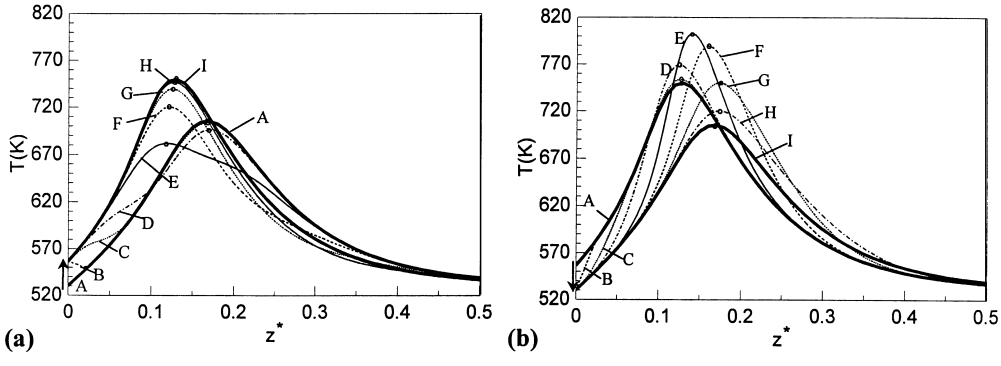

Fig. 2. Transient axial temperature profiles for different t^* values: A-0; B-10; C-50; D-100; E-200; F-300; G-400; H-500; I-1000, obtained with the PH1DT model for a fixed bed packed with pure catalyst, by changing the feed temperature: (a) + 5% ($T_o = 530 \rightarrow 557$ K); (b) − 5% ($T_o = 557 \rightarrow 530$ K).

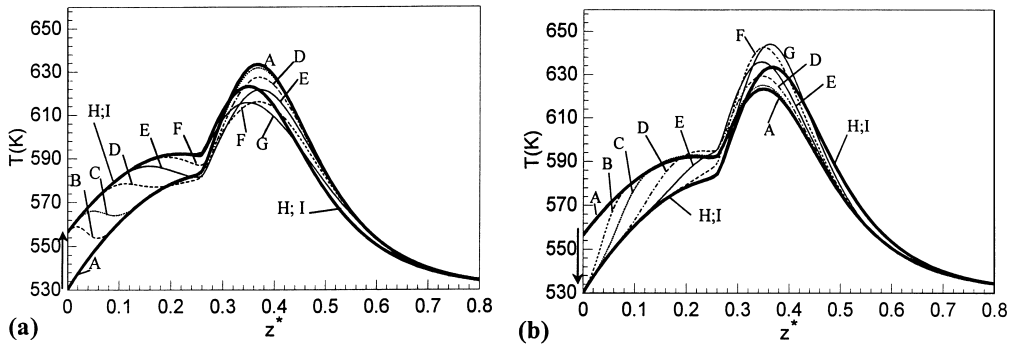

Fig. 3. Transient axial temperature profiles for different t^* values: A-0; B-50; C-100; D-200; E-300; F-400; G-500; H-700; I-1000, obtained with PH1DT model for a fixed bed with two different catalytic zones, by changing the feed temperature: (a) + 5% ($T_o = 530 \rightarrow 557$ K); (b) − 5% ($T_o = 557 \rightarrow 530$ K).

for higher operating feed temperatures, as in the case of the uniform bed. In fact, the global bed temperature will be increased but the maximum value can be lowered. In this context, the reactor with a partially diluted bed shows increased wrong-way behavior, since the final response to a positive change in the inlet temperature is negative.

A step down in feed temperature (Fig. 3(b)) results in a transient increase in both maxima of the reactor temperature (one in each catalytic zone) as the hot spots move downstream, followed by a temperature drop. The high transient hot spots (curves F and G), are due to the increased methanol concentration contacting the previous hot spot zones before they are cooled. In fact, in the first part of the reactor, the methanol has a lower consumption for the new lower feed temperature, leading then to higher concentrations downstream. The same type of behavior described above for partially diluted beds can also be observed when the feed temperature decreases. If we compare, in this case, the initial and final steady-state profiles (curves A and I, Fig. 3(b)) a higher hot-spot temperature is detected. This is not observed in the uniform bed, where for a decrease of the inlet temperature a lower maximum in the final steady-state is expected (Fig. 2(b)). The wrong-way behavior is a result of appreciable heat transfer taking place between the two phases before considerable reaction takes place. In the diluted part of the two-zone bed, the reaction time scales are increased and hence, substantial heat transfer takes place between the two phases before significant reaction takes place. Therefore, this system with diluted catalyst exhibits increased wrong-way behavior, even if the transient hot spots are lower than in the one-zone bed, which points out a reduction of the sensitivity of the system. In fact, while in the uniform bed a positive/negative change in the inlet temperature also leads to a positive/negative change in the final hot spot temperatures, for the partially diluted bed, the final steady-state response to a positive change in the inlet gas temperature is negative and is positive for a negative inlet change.

Fig. 4(a) shows the dynamic responses for a stronger decrease in feed temperature (from 583 to 530 K), revealing a more pronounced increase in the final steady-state hot spot, when compared to Fig. 3(b). These results reinforce the specific characteristics of the diluted bed when submitted to thermal perturbations.

Using a heterogeneous model, $HT1DT_d$, the same feature can be observed in Fig. 4(b), which also points out more significant differences on the transient predictions of both models than on the steady-state ones. These differences can also be explained by the theory of time scales or characteristic times. In the pseudo-homogeneous model, PH1DT, the fluid–solid resistances are neglected ($\tau_{hf} = 0$), being then the relative magnitude of the reaction time scale in respect to the heat transfer time scale higher than in the case of the heterogeneous model, HT1DT, where those resistances are accounted for. Thus, the homogeneous model must predict a stronger wrong-way behavior compared to the heterogeneous model that uses finite heat transfer time scale between the gas and the solids. In Fig. 5, the results of Fig. 4(a) are represented in a three-dimensional plot, which clearly shows the wrong-way behavior associated to the heat wave travelling along the catalytic bed, after a decrease in feed temperature, it being possible to observe that the final steady-state is preceded by the development of higher maxima temperatures.

In a previous work (Quina & Quinta Ferreira, 1999a) we have shown that for certain inlet operating conditions ($C_{M,o}$, T_o) the hot-spot temperature can follow a runaway process. This is the case for $C_{M,o} = 3.4$ mol/m^3 and $T_o = 530$ K. Therefore, we have changed the inlet methanol concentration from 2.4 to 3.4 mol/m^3 for a fixed feed temperature of 530 K, in order to determine the dynamic behavior of the system. According to these results, after $t^* \geqslant 1000$ the temperature runs away (Fig. 6(a)) leading to a severe deactivation of the catalyst and strong negative consequences for the desired product (curves I and J, Fig. 6(b)), which may even disappear due to the secondary reaction. In fact, in this system with consecutive

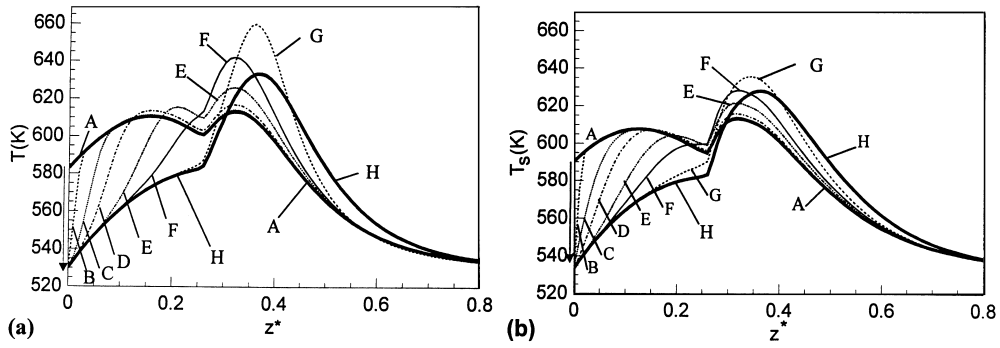

Fig. 4. Dynamic response to a step down in feed temperature (583 → 530 K). Axial temperature profiles for different dimensionless times, $t^* =$: A-0; B-10; C-50; D-100; E-200; F-300; G-500; H-1000: (a)- PH1DT model; (b) $HT1DT_d$ model.

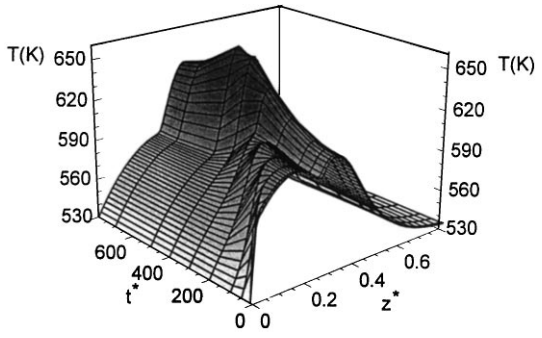

Fig. 5. Dynamic response to a step down in feed temperature (583 → 530 K), for the PH1DT model.

reactions, the increase of feed temperature does not lead necessarily to a higher yield.

When the wall temperature, T_w, is step changed from 530 to 583 K, Fig. 7 shows an overall increase in the temperature inside the reactor. Since the effect of T_w extends into all the reactor length, the initial steady-states profiles are immediately changed. For a step-up change, one can observe in Fig. 7(a) two hot spots (one in each zone) for some dimensionless times due to the existence of two different catalytic zones. Fig. 7(b) shows some transient profiles after a step down in the wall temperature. Curves B and C are under the initial steady-state (curve A) for all axial positions, but after $t^* = 200$ (Curve D) a pronounced hot spot is developed on the second zone of the reactor. However, afterwards this hot spot decreases until a final steady-state is reached (curve I). Those intermediate higher temperatures, also showing a wrong-way behavior, are due to the increased methanol concentration (the methanol has a lower consumption near the entrance for the new lower wall temperature) which contacts the downstream hot zones leading to higher reaction rates before they are cooled by the lower wall temperature. One can also conclude that the wall temperature has a stronger effect on the system, when compared with the feed temperature, as it had been predicted through the sensitivity analysis of the present system (Quina & Quinta Ferreira, 1999b).

For a simultaneous perturbation in feed and wall temperatures, Fig. 8(a) and (b) show some transient axial temperature profiles. Immediately after the disturbance, the initial steady-state is moved in the vertical due to the wall temperature change, this effect being stronger on the initial part of the reactor, because of the feed temperature effect. When both temperatures increase (T_o and T_w) from 530 to 583 K, the final steady-state has only one hot spots (curve J, Fig. 8(a)) and when they decrease higher intermediate hot spots can be observed (curves F–H, Fig. 8(b)), showing again the wrong-way behavior of the diluted bed. Moreover, in these cases, when T_o and T_w are disturbed simultaneously, the hot spot(s) can move significantly upstream or downstream in the reactor.

The inverse response of the system can also be observed for ramp variations, as shown in Figs. 9 and 10. When the feed and wall temperatures increase linearly with time until $t^* = 800$ and then decrease, the displacement of the thermal wave can be observed in the three-dimensional plot of Fig. 9(a). Fig. 9(b) clearly shows that the hot-spot temperature continues to increase until $t^* = 1350$ (for $z^* = 0.32$) decreasing only afterwards. Fig. 10 show the opposite situation, when the feed and wall temperatures decrease linearly with time until $t^* = 800$, and then increase. The wrong-way behavior is detected by the decrease of the hot spot until $t^* = 1050$ (for $z^* = 0.37$, Fig. 10(b)). It is also interesting to note that there are some axial positions (for instance $z^* = 0.5$) for which the temperature remains nearly constant along the time (Fig. 9(b) and 10(b)), without reflecting the thermal disturbance introduced in the system.

Finally, Fig. 11 shows axial profiles of the solid temperature predicted with $HT1D_d$ ($\lambda_{m,i} = 0$) and $HT1DT_{dc}$ ($\lambda_{m,i} = 10$) models. In Fig. 11-I one can see the initial steady-states for $T_o = 530$ K, in Fig. 11-II the transient profiles for a particular time of $t^* = 300$, after a step change in feed temperature from 530 to 557 K; and in Fig. 11-III, the final steady-states for $T_o = 557$ K. In all the situations, when the intraparticle convection is taken into account ($\lambda_{m,i} = 10$) the axial temperature before the hot spot is higher than when $\lambda_{m,i} = 0$. This is due to the

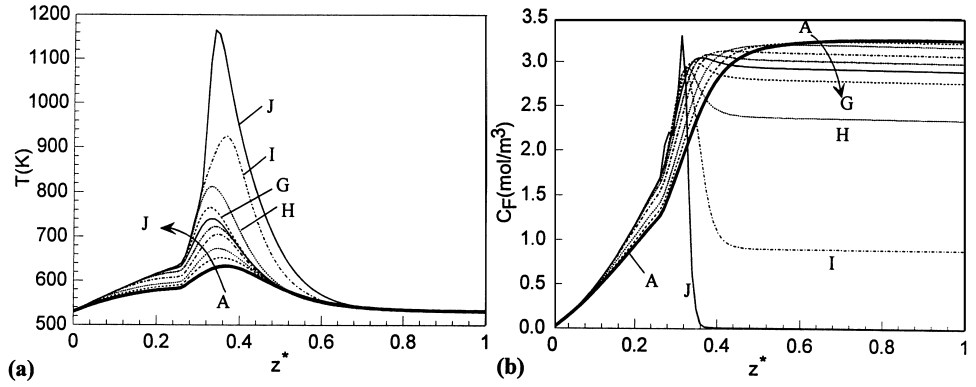

Fig. 6. Transient axial profiles for different t^* values: A-0; B-50; C-100; D-200; E-300; F-400; G-500; H-700; I-1000, J- 1200, obtained with PH1DT model for a fixed bed with two different catalytic zones, by changing the feed methanol concentration from 2.4 to 3.4 mol/m^3 (+ 41%): (a) temperature; (b) formaldehyde concentration.

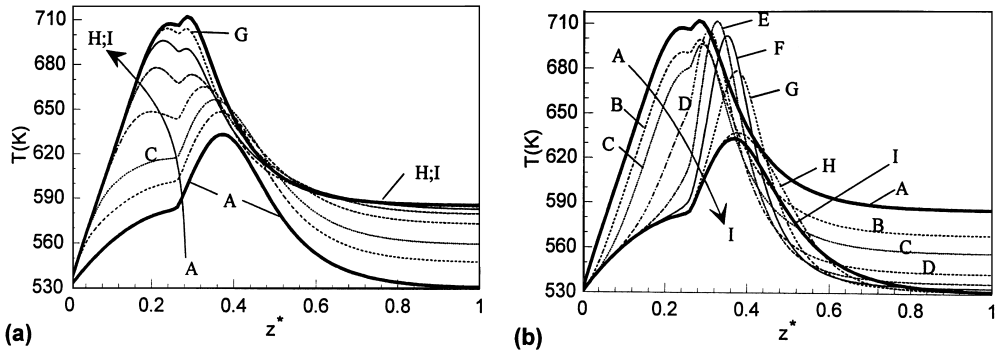

Fig. 7. Transient axial temperature profiles for different t^* values: A-0; B-50; C-100; D-200; E-300; F-400; G-500; H-700; I-1000, obtained with PH1DT model for a fixed bed with two different catalytic zones, by changing the wall temperature: (a) + 10% ($T_w = 530 \rightarrow 583$ K); (b) -10% ($T_w = 583 \rightarrow 530$ K).

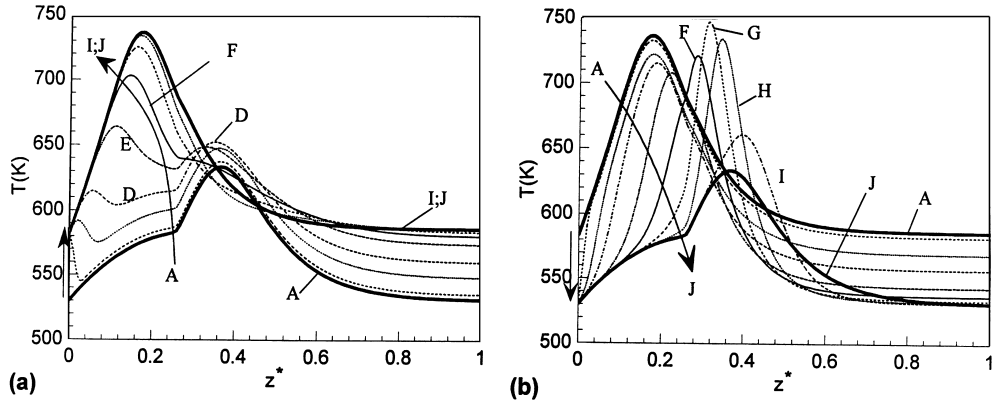

Fig. 8. Transient axial temperature profiles for different t^* values: A-0; B-10; C-50; D-100; E-200; F-300; G-400; H-500; I-700; J = 1000, obtained with PH1DT model for a fixed bed with two different catalytic zones, by changing T_o and T_w: (a) + 10% ($T_o = T_w = 530 \rightarrow 583$ K); (b) − 10% ($T_o = T_w = T_w = 583 \rightarrow 530$ K).

additional mass transport, which increases the reaction rate and the heat, released by the reaction, leading to higher bed temperatures. In fact, increasing $\lambda_{m,i}$ (from 0 to 10) the reaction time scale decreases due to the increase in the reaction rate provoked by a higher concentration of the reactants inside the catalyst, through the additional convective transport. This will affect the wrong-way behavior leading to higher transient maximum temperatures, when compared with those obtained with the model which considers the internal diffusion as

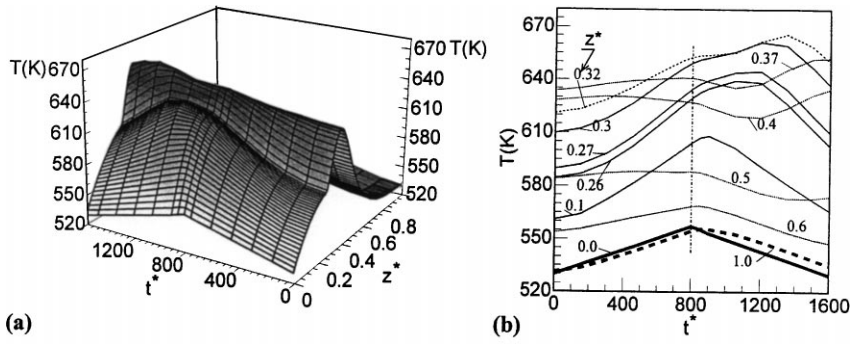

Fig. 9. Dynamic response to a positive ramp in feed and wall temperatures during $0 \leqslant t^* \leqslant 800$, followed by a negative ramp during $800 \leqslant t^* \leqslant 1600$, for the PH1DT model: (a) 3-D plot; (b) Temperature versus dimensionless time for different axial positions.

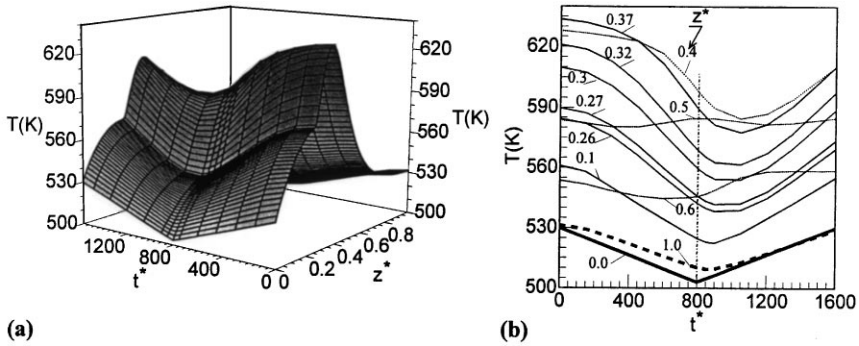

Fig. 10. Dynamic response to a negative ramp in feed and wall temperatures during $0 \leqslant t^* \leqslant 800$, followed by a positive ramp during $800 \leqslant t^* \leqslant 1600$, for the PH1DT model: (a) 3-D plot; (b) Temperature versus dimensionless time for different axial positions.

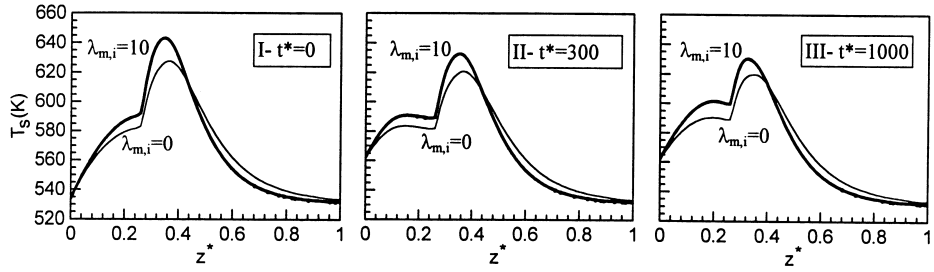

Fig. 11. Axial profiles of the catalyst temperature predicted with $HT1D_d$ ($\lambda_{m,i} = 0$) and $HT1DT_{dc}$ ($\lambda_{m,i} = 10$) models. I- initial steady-state for $T_o = 530\ K$; II- transient profile for $t^* = 300$, after a step change in feed temperature from 530 to 557 K; III- final steady-state for $T_o = 557\ K$.

the only transport mechanism inside the catalyst particles ($\lambda_{m,i} = 0$).

4. Conclusions

The start-up and the transient behavior of a fixed-bed reactor is analyzed by using pseudo-homogeneous and heterogeneous one-dimensional models, and in both cases axial dispersion terms were included, which are advantageous for the dynamic simulations.

During the start-up period, the high thermal capacity of the catalytic bed leads to a slower propagation of the thermal waves in relation to the mass waves, which leads to the development of sharp mass fronts.

The orthogonal collocation on finite elements was used for the spatial discretization of the partial differential model equations, showing good results when an appropriate number of intervals is used. Moreover, in our case, due to the different activities of the catalytic bed, the process variables also show abrupt variations in the transition zone, and therefore a higher number of finite elements were concentrated there in order to avoid numerical oscillations.

When step or ramp changes in feed temperature, in wall temperature and in feed and wall temperatures

simultaneously were imposed in the system, it was possible to observe the wrong-way behavior of the temperature profiles and in some cases a pronounced displacement of the hot spot was detected. The step changes in the feed concentration require a higher CPU time (due to the sharp mass fronts), and during the transient period the hot spot has practically the same location.

The partially diluted two-zone bed reveals an increased wrong-way behavior, since in this case the final response to a positive change in the inlet temperature is negative and for a negative change in the feed temperature, the steady-state response is positive. This is indeed a very important feature to account for on diluted beds in what concerns the design and control of these systems, since it will be an unexpected situation if the analysis is based on the behavior of a uniform packing. In fact, in the one-zone bed, even if the maximum transient temperatures can be farther from the departure hot spots in the wrong direction, one can observe that a positive/negative change in the inlet temperature leads also to a positive/negative change in the final steady-state hot-spot temperatures, which is not the case of the two-zone bed. For some perturbations the temperature can runaway drastically, which is highly undesirable for the process, because the desired product may be oxidized and the catalyst can be deactivated in a very severe way.

The predictions of the heterogeneous model and the pseudo-homogeneous model are quite similar for moderate steady-state conditions, being the differences more pronounced in the transient regime. The pseudo-homogeneous model assumes the same local temperature for the gas and the solids and hence, the time scale for heat transfer between the two phases is zero, whereas reaction time scales is finite. Thus the pseudo-homogeneous model must predict a stronger wrong-way behavior, when compared to the heterogeneous model that uses a finite heat transfer time scale between the gas and the solid.

When the intraparticle convection is taken into account in the heterogeneous model, the transient hot spots are higher than the ones observed when diffusion is the only intraparticle mechanism of transport.

Notation

A_p specific particle area, m^{-1}

a_v specific particle area (referred to the reactor volume) $[=(1-\varepsilon_b)A_p]$, m^{-1}

B_j adiabatic temperature rise of reaction j, $[=(-\Delta H)_j C_{M,o}/\rho_f C_f T_o]$

$C_{i,b}$ concentration of component i in the bulk phase, mol/m^3

$C_{M,o}$ feed methanol concentration, mol/m^3

Cp_f fluid heat capacity J/kg K

Cp_s solid heat capacity, J/kg K

d_{pe} equivalent diameter of the particle (volume/area), m

d_t diameter of the reactor tube, m

Da damköhler number $(=L\rho_b R_{1,o}/u_o C_{M,o})$

$D_{e,i}$ effective diffusivity of component i in the catalyst, m^2/s

D_{ea} effective axial diffusivity, m^2/s

$f_{i,b}$ dimensionless concentration of component i at the bulk $(=C_{i,b}/C_{M,o})$

$f_{i,p}$ dimensionless concentration of component i at the particle $(=C_{i,p}/C_{M,o})$

$f_{i,s}$ dimensionless concentration of component i at the catalyst surface, $(=C_{i,s}/C_{M,o})$

$f_{i,o}$ dimensionless concentration of component i at the inlet conditions, $(=C_{i,o}/C_{M,o})$

h_f film heat transfer coefficient, J/m^2s K

$k_{f,i}$ film mass transfer coefficient for component i, m/s

L reactor length, m

Nf_h number of film heat transfer units, $(=h_f a_v L/u_o \rho_f Cp_f)$

Nf_i number of film mass transfer units $(=k_{f,i} a_v L/u_o)$

N_w number of wall heat transfer units $(=4UL/d_t \rho_f Cp_f u_o)$

P total pressure, atm

P_{CH_2O} formaldehyde partial pressure, atm

Pe_{ha} axial heat Peclet number $(=Lu_o \rho_f Cp_f/\lambda_{ea})$

$Pe_{ha}(d_{pe})$ axial heat Peclet number based on particle diameter $(=d_{pe} u_o \rho_f Cp_f/\lambda_{ea})$

Pe_{ma} axial mass Peclet number $(=Lu_o/D_{ea})$

$Pe_{ma}(d_{pe})$ axial mass Peclet number based on particle diameter $(=d_{pe} u_o/D_{ea})$

P_o inlet pressure, atm

R_j reaction rate, mol/s kg_{cat}

R_p half-thickness of the slab catalyst, m

$\Re_j^s$ dimensionless reaction rate j, at catalyst surface conditions $(=R_j^s/R_{1,o})$

$\Re_j^p$ dimensionless reaction rate j, inside the catalyst, $(=R_j^p/R_{1,o})$

r_p particle spatial coordinate, m

r_p^* dimensionless particle coordinate, $(=r_p/2R_p)$

$R_{1,o}$ main reaction rate at feed conditions, mol/kg s

R_j^p rate of disappearance by reaction for component j inside the catalyst, mol/s kg_{cat}

R_j^s rate of disappearance by reaction for component j at catalyst surface conditions, mol/s kg_{cat}

t time, s

t^* dimensionless time $(=t/\tau)$

T absolute temperature, K

T_o feed temperature, K

T_s catalyst temperature, K

T_w wall temperature, K

U overall heat transfer coefficient, J/m^{2}s K
u_i interstitial fluid velocity, m/s
u_o superficial fluid velocity, m/s
v_o intraparticle fluid velocity, m/s
Y_M methanol molar fraction ($=F_M/\sum F_i$)
z reactor axial coordinate, m
z^* dimensionless reactor axial coordinate, (z/L)

Greek symbols

$\alpha_{i,j}$ stoichiometric coefficient of component i, at j reaction
ΔH reaction heat, J/mol
ε porosity
η_j effectiveness factor
$\phi_{i,o}$ Thiele modulus referred to the inlet conditions ($=R_p\sqrt{\rho_p R_{1,o}/D_{e,i}C_{M,o}}$)
θ dimensionless temperature ($=T/T_o$)
θ_b dimensionless bulk temperature ($=T_b/T_o$)
θ_o dimensionless feed temperature ($=T_o/T_o$)
θ_s dimensionless catalyst temperature ($=T_s/T_o$)
θ_w dimensionless wall temperature ($=T_w/T_o$)
λ_{ea} axial effective thermal conductivity, J/ms K
$\lambda_{m,i}$ intraparticle mass Peclet number of component i ($=v_o R_p/D_{e,i}$)
ρ density, kg/m^3
τ space time for the fluid ($=L/u_i$)
τ_c time scale for intraparticle convection ($=\varepsilon_p R_p/v_o$)
$\tau_{d,i}$ time scale for pore diffusion within the pellet ($=\varepsilon_p R_p^2/D_{e,i}$)
τ_h space time for the thermal wave ($=\tau(1-\varepsilon_b)\rho_s Cp_s/\varepsilon_b\rho_f Cp_f$)
τ_{hf} film heat transfer space time, ($=\rho_f Cp_f\varepsilon_b/h_f a_v$)
τ_{hl} lumped space time for the thermal wave ($=\tau[(1-\varepsilon_b)\rho_s Cp_s+\varepsilon_b\rho_f Cp_f]/\varepsilon_b\rho_f Cp_f$)
τ_r reaction time scale ($\varepsilon_b C_{M,o}/\rho_b R_{1,o}$)

Subscripts

1, 2 reactions 1 and 2
b bulk conditions in the fluid phase
d diffusion
dc diffusion and convection
F formaldehyde
i component i
j reaction j ($=1, 2$)
M methanol
o inlet conditions
p particle
s particle surface
w wall

Superscripts

$*$ hot-spot conditions or normalized variables
f fluid
p particle
s particle surface

References

Almeida-Costa, C. A., Quinta Ferreira, R. M., & Rodrigues, A. E. (1994). Wrong-way behavior in packed bed reactors with "large-pore" catalysts. *Chemical Engineering Science*, *49*(24B), 5571–5583.

Alvarez, J., Romagnoli, J., & Stephanopoulos, G. (1981). Variable measurement structures for the control of a tubular reactor. *Chemical Engineering Science*, *36*(10), 1695–1712.

Bucalá, V., Borio, D. O., Romagnoli, J. A., & Porras, J. A. (1992). Influence of a cooling design on fixed-bed reactors dynamics. *A.I.Ch.E. Journal*, *38*(12), 1990–1994.

Chen, Y. C., & Luss, D. (1989). Wrong-way behavior of packed-bed reactors: Influence of interphase transport. *A.I.Ch.E. Journal*, *35*(7), 1148–1156.

Crider, J., & Foss, A. (1966). Computational studies of transients in packed tubular chemical reactors. *A.I.Ch.E. Journal*, *12*(3), 514–522.

Dente, M., & Collina, A. (1965). Cinetica dell'ossidazione del metanolo a formaldeide con catalizzatore a base di ossidi di Fe e Mo - Nota III. *La Chimica e L'Industria*, *47*(8), 821–829.

Dente, M., Collina, A., & Pasquon, I. (1966). Verifica di un Reattore Tubolare per la Ossidazione del Metanolo a Formaldeide. *La Chimica e L'Industria*, *48*(6), 581–588.

Ferguson, N., & Finlayson, B. (1974). Transient modelling of a catalytic converter to reduce nitric oxide in automobile exhaust. *A.I.Ch.E. Journal*, *20*, 539–550.

Hansen, K. (1971). Analysis of transient models for catalytic tubular reactors by orthogonal collocation. *Chemical Engineering Science*, *26*, 1555–1569.

Hansen, K. (1973). Simulation of the transient behaviour of a pilot plant fixed bed reactor. *Chemical Engineering Science*, *28*, 723–734.

Harris, T. J., MacGregor, J. F., & Wright, J. D. (1980). Optimal sensor localisation with an application to a packed bed tubular reactor. *A.I.Ch.E. Journal*, *26*(6), 910–916.

Il'in, A., & Luss, D. (1992). Wrong-way behavior of packed-bed reactors: Influence of reactant adsorption on support. *A.I.Ch.E. Journal*, *38*, 1609–1617.

Il'in, A., & Luss, D. (1993). Wrong-way behavior of packed-bed reactors: Influence of an undesired consecutive reaction. *Industrial and Engineering Chemistry Research*, *32*, 247–252.

Kulkarni, M. S., & Dudukovic, M. P. (1996). Dynamics of gas phase and solid phase reactions in fixed bed reactors. *Chemical Engineering Science*, *51*(11), 3083–3088.

Kulkarni, M. S., & Dudukovic, M. P. (1998). Periodic operation of asymmetric bidirectional fixed-bed reactors with temperature limitations. Industrial & Engineering Chemistry Research, 37(3), 770–781.

Lopéz-Isunza, H. F. L. (1983). Steady-state and dynamic behaviour of an industrial fixed bed catalytic reactor. Ph.D. thesis, Imperial College, London.

Madsen, N., & Sincovec, R. (1975). PDECOL: General collocation on finite elements. *Chemical Engineering Science*, *30*, 587–596.

McGreavy, C., & Naim, H. (1977). Reduced dynamic model of a fixed bed reactor. *Canadian Journal Chemical Engineering*, *55*, 326–332.

Metha, P., Sams, W., & Luss, D. (1981). Wrong-way behavior of packed-bed reactors I- The pseudo-homogeneous model. *A.I.Ch.E. Journal*, *27*, 234–246.

Pinjala, V., Chen, Y. C., & Luss, D. (1988). Wrong-way behavior of packed-bed reactors: II Impact of thermal dispersion. *A.I.Ch.E. Journal*, *34*, 1663–1672.

Quina, M.J., Quinta Ferreira, R. (1998) Simulation of a fixed bed reactor with two catalytic zones: Numerical methods. Proceedings of second meeting on numerical methods for differential equations, Coimbra.

Quina, M. J., & Quinta Ferreira, R. (1999a). Thermal runaway conditions of a partially diluted catalytic reactor. *Industrial & Engineering Chemistry Research*, *38*, 4615–4623.

Quina, M. J., & Quinta Ferreira, R. (1999b). Model comparison and sensitivity analysis for a fixed bed reactor with two catalytic zones. *Chemical Engineering Journal*, *75*, 149–159.

Quinta Ferreira, R., Costa, A. C., & Rodrigues, A. E. (1992). Dynamic Behavior of fixed-bed reactors with large-pore catalysts: A bidimensional heterogeneous diffusion/convection model. *Computers and Chemical Engineering*, *16*(8), 721–751.

Quinta Ferreira, R. M., Costa, A. C., & Rodrigues, A. E. (1996). Effect of intraparticle convection on the transient behavior of fixed-bed reactors: finite differences and collocation methods for solving unidimensional models. *Computers & Chemical Engineering*, *20*(10), 1201–1225.

Sharma, C., & Hughes, R. (1979a). The behaviour of an adiabatic fixed bed reactor for the oxidation of carbon monoxide I. *Chemical Engineering Science*, *34*, 613–624.

Sharma, C., & Hughes, R. (1979b). The behaviour of an adiabatic fixed bed reactor for the oxidation of carbon monoxide II. *Chemical Engineering Science*, *34*, 625–634.

Sinai, J., & Foss, A. S. (1970). Experimental and computational studies of the dynamic of a fixed bed chemical reactor. *A.I.Ch.E. Journal*, *16*(4), 658–669.

Van Doesburg, H., & De Jong, W. (1976). Transient behaviour of an adiabatic fixed-bed reactor methanator I. *Chemical Engineering Science*, *31*, 45–51.

Verwijs, J. W., Köster, P. H., van den Berg, H., & Westerterp, K. R. (1995). Reactor operating procedures for the start-up of continuously operated chemical plants. *A.I.Ch.E. Journal*, *41*(1), 148–158.

Verwijs, J. W., van den Berg, H., & Westerterp, K. R. (1992). Start-up of an industrial adiabatic tubular reactor. *A.I.Ch.E. Journal*, *38*(12), 1871–1880.

Windes, L., Schwedock, M., & Ray, H. (1989). Steady-state and dynamic modelling of a packed bed reactor for the partial oxidation of methanol to Formaldehyde. I. Model development.. *Chemical Engineering Communications*, *78*, 1–43.

Zheng, Y., & Gu, T. (1996). Analytical solution to a model for the start-up period of fixed-bed reactors. *Chemical Engineering Science*, *51*(15), 3773–3779.